Synthesis of Zinc Stannate Powder by Solid State Route and Molten Salt Synthesis Method and their characterization

A thesis submitted in partial fulfillment

Of the requirements for the degree of

Bachelor of Technology

By

Prabin Kumar Seth

(111CR0587)

Under the guidance of

Prof. Ranabrata Mazumder

Department of Ceramic Engineering

National Institute of Technology

Rourkela – 769 008

NATIONAL INSTITUTE OF TECHNOLOGY

ROURKELA

CERTIFICATE

This is to manifest that this project report ennobled, "***Synthesis of Zinc Stannate Powder by Solid State Route and Molten Salt Synthesis Method and their characterization***", being submitted by Mr. ***Prabin Kumar Seth*** (Roll No. ***111CR0587***), Department of Ceramic Engineering, National Institute of Technology, Rourkela, as partial fulfillment of the requirements for the Degree of Bachelor of Technology in Ceramic Engineering is a record of unquestionable work carried out by him under my guidance. The results of investigations introduced in this report have been verified and found to be more than satisfactory.

To the best of my cognition, the matter embodied in the thesis has not been presented to any other University/Institute for the award of any Degree or Diploma.

Prof. Ranabrata Mazumdar

Associate Professor

Department of Ceramic Engineering

National Institute of Technology, Rourkela.

Acknowledgement

With a feeling of great pleasure and deep sense of gratitude, I would like to express my thankfulness to my guide **Prof. Ranabrata Mazumder,** Dept. of Ceramic Engineering, NIT, Rourkela for his excellent support and guidance throughout the duration of my work and in the preparation of report. I received excellent academic training from him. Thank you sir for your valuable advice and inspiration.

I express my deep gratitude to Prof. S.K. Pratihar, Head of the Department of Ceramic Engineering, NIT, Rourkela for providing me all the necessary facilities in the department.

I express my thankfulness to all the faculty members for their kind help extended towards me.
I express my deep gratitude and sincere thanks to Mr Sreeram Abhinay, Mr G.Jayarao for their constant help and support during my project work.

I am very thankful to all my friends specially Mr. Hitesh Ku Biswal, Mr. Rahul Sahoo, Mr. Artatrana Tandi, Mr. Shiba Shankar Satapathy and Mr. Utsarga Choudhury for their support and encouragement.

I would take this opportunity to express my thanks to laboratory Members of Department of Ceramic Engineering, N.I.T. Rourkela.
Finally I am grateful to my parents and I would like to share this moment of happiness with them.

27th June 2015 Prabin Kumar Seth

Abstract

The solid state route and molten salt synthesis method was successfully employed to synthesize Zn_2SnO_4 powder. ZnO and SnO_2 were used as starting material. For molten salt synthesis NaCl-KCl salt system was used as reaction media. The different processing parameters e.g. salt quantity, heat treatment temperature, holding time were varied to study the phase formation. As synthesized powder sample was characterized using X-ray diffraction (XRD) which reveals the phase purity of zinc stannate synthesized from solid state route while a few percentage of phase formation has occurred in molten salt synthesis method. The particle size and morphology of the zinc stannate powder was studied using FESEM and particle size analyzer. The optical property was studied using UV-visible spectroscopy.

Keywords : Zn_2SnO_4, Solid State Route, Molten Salt Synthesis, FESEM, UV-Vis Spectroscopy.

CONTENTS

List of Figures

CHAPTER – 1

INTRODUCTION

1. INTRODUCTION

Zinc stannate (ZTO) is an n-type semiconducting complex oxide with low visible absorption, a band gap of 3.6 eV and electron mobility of 10-15 cm^2 V^{-1} s^{-1} [1]. It has a typical 2-4 cubic inverse spinal structure. In functional coating, electrode for lithium batteries Zinc Stannate has wide application. Zinc stannate is a promising candidate as anode for dye-sensitized solar cells (DSSCs), the application of ZTO as anode material for dye-sensitized solar cells (DSSC) has attracted extensive research [2]. It has been also used as chemical sensor and photocatalyst [3]. Methods such as solid state synthesis, chemical vapor deposition, thermal evaporation, hydrothermal method, mechanical grinding, high temperature calcination, and sol−gel technique have been used to fabricate Zinc stannate [4]. The traditional solid state synthesis of ZTO involves the reaction between the starting material ZnO and SnO_2 which requires prolonged heat treatment at high calcination temperature of above 1000^oC and in many case this cause the loss of zinc due to its high volatile nature and it results in the formation of multiple products and degradation of microstructural properties [5-6]. The extensively used method for the synthesis of Zinc stannate is thermal evaporation which suffers from low yield and severe experimental condition.

Molten salt synthesis is powder preparation method used to synthesize ceramic powder at low temperature by using eutectic mixture of salt such as NaCl-KCl, NaOH-KOH as reaction media and heating the reactants above the eutectic temperature of salt system. This method involves lower temperature of reaction to avoid the loss of volatile material and degradation of microstructure at high calcination temperature. This method is also used to increase the rate of reaction and degree of homogeneity [7].

1.1 **Crystal Structure**

Zn_2SnO_4

Zn_2SnO_4 possess 2-4 inverse cubic spinel structure with the space group of Fd3m. The inverse spinel structure is represented by a formula $BABO_4$ where A is tetravalent and B is divalent. Zinc stannate correspond to the 4-2 form where Zn carries +2e charge and Sn carries +4e charge

which is written as $(Zn^{2+})[Sn^{4+}Zn^{2+}]O_4$ [8].

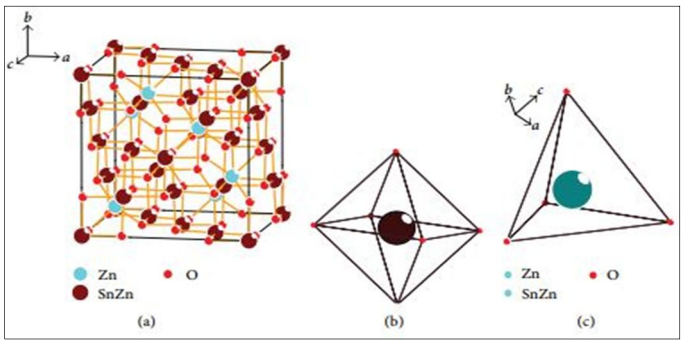

Figure 1 Schematic representation of the crystal structure of "inverse spinal" Zn_2SnO_4 (b) Octahedral coordinated "SnZn" cation. (c) Tetrahedral coordinated Zn atom [9].

ZnO

ZnO poses various crystal structure. It is an II-IV group of semiconductor most of which crystallize to hexagonal wurtzite or cubic zinc blende structure. In crystal structure there is tetrahedral coordination, at the corners of a tetrahedron sites each anion is bounded by four cations, and vice versa. The bonding nature is of sp^3 covalent [10].

The ionicity of ZnO which is an II–VI compound semiconductor resides between the ionicity of covalent and ionic semiconductors. ZnO poses three different type of crystal structures such as wurtzite, zinc blende, and rocksalt.

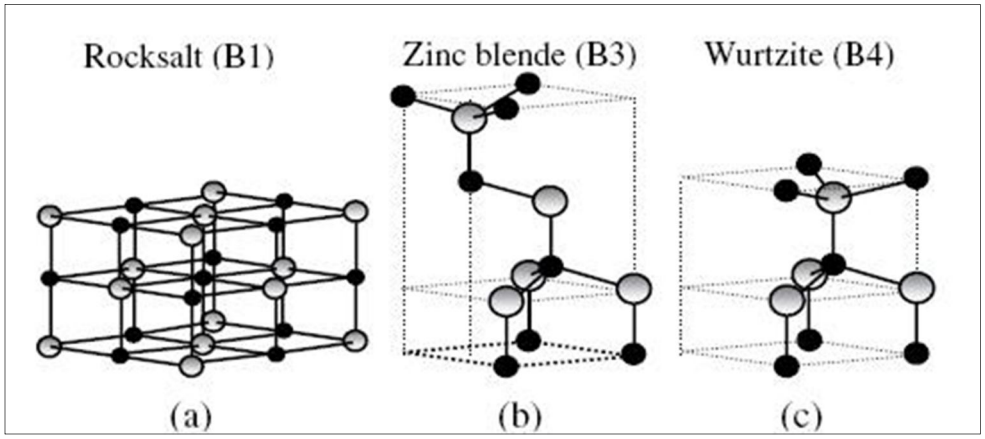

Figure 2 Representation of crystal structures of ZnO: (a) cubic rock salt, (b) cubic zinc blende, and (c) hexagonal wurtzite. Shaded black and gray spheres denote O and Zn atoms, respectively.

SnO_2

SnO_2 possess a rutile (Cassiterite) crystal structure with tetragonal unit cells and have a group space symmetry of P42/mnm. In the SnO_2 matrix tin atoms are six fold coordinated to three fold coordinated oxygen atoms. The lattice parameter for SnO_2 are a = b = 4.731 A ˚ and c = 3.189 A˚, The figure represent a unit cell [11].

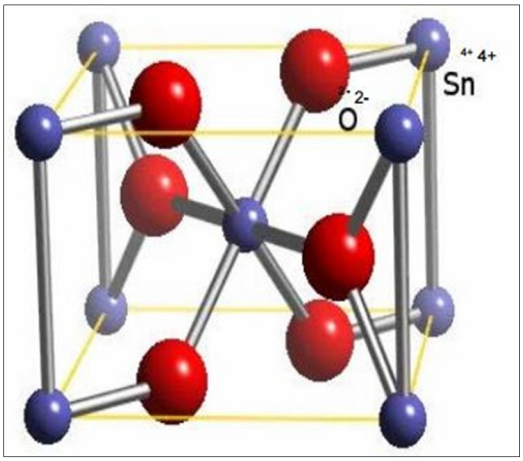

Figure 3 SnO_2 Cassiterite Structure

CHAPTER – 2

LITERATURE REVIEW

Various works has been done on zinc stannate. **Chen et al.** reported the hierarchical Zn_2SnO_4 nanostructures synthesis by a single-step hydrothermal route where pure Zn_2SnO_4 phase can be obtained by hydrothermal route with strong and narrow peaks. They measured ethanol sensing properties of Zn_2SnO_4 nanostructure.

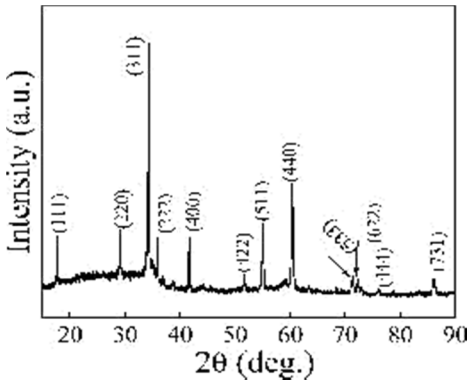

Figure 4 .XRD pattern of $Zn2SnO_4$ as-synthesized by Hydrothermal method [12]

The band gap of as synthesized Zn_2SnO_4 was estimated to be 3.56 eV by extrapolating a tangent line in tauc plot. The tauc plot is square root of the Kubelka Munk functions (y axis) against hυ photon energy (x axis), the band gap is lower than the band gap value of bulk Zn_2SnO_4 (3.6eV) [12].

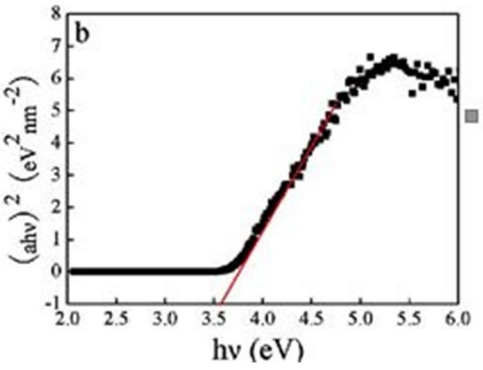

Figure 5. $(\alpha h\nu)^2$ vs hν curve [12]

Sepelak et al. studied the synthesis of Zn_2SnO_4 nanoparticles by one-step mechanochemical processing where the binary oxide precursors were processed and fired at recommended

temperature have an average particle size of 26 nm. Synthesis method involves mixing of precursors ZnO and SnO_2 in molar ratio of 2:1. Then the mixture is milled for many time and prefired at 1100^oC for one day and finally sintered at 1100^oC. The route is simple as there is no need of subsequent calcination. If the milling time is more than 1 hr changes in milled powder is observed from XRD peaks. TEM micrograph revealed that the synthesize Zinc Stannate consist of nano particles ranging from 5nm to 50 nm. From TEM result it was concluded that the synthesis of Zinc Stannate nanoparticles possess a non-uniform configuration consist of an ordered core covered by a shell region of disordered surface [13]. Synthesis of spherical Zn_2SnO_4 particles was successful by microwave-assisted combustion method. Zinc nitrate and tin nitrate are used as precursor and glycine is used as fuel. In this work **Nehru et al.** [14] reported the confirmation of face-centered cubic spinel structure of Zn_2SnO_4 from XRD pattern. The average particle size of nano crystalline powder was calculated to be 50 to 60 nm. The advantage of microwave assisted combustion method is without the treatment at high temperature crystalline powders having grain and high purity can be obtained. The figure below shows XRD pattern of intensities of Zn_2SnO_4 formed when different amount of fuel were used.

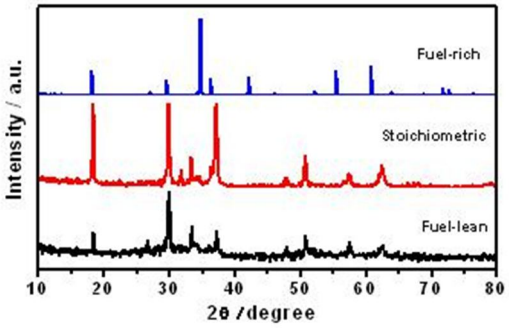

Figure 6.The XRD patterns of glycine used Zn_2SnO_4 [14]

The band gap value was obtained from the tauc plot. Tauc's relationship $(\alpha h\upsilon)^2=A(h\upsilon - E_g)$ where α, h denotes absorption coefficient and the Planck's constant, υ denotes frequency of the incident photon respectively. Eg denotes the band gap (optical energy) and A is simply a constant. By extrapolating the $(\alpha h\upsilon)^2$ (y-axis) versus hυ (x-axis) the band gap value is estimated. An absorption energy corresponding to Eg = 3.5 eV is obtained by Plotting $(\alpha h\upsilon)^2$ and extrapolating linear portion of curve to the axis of photon energy [15]. DSC/TGA investigation of mixture of ZnO and SnO_2 shows 0.42% weight loss upto 1200 and small exothermic peak at 878^oC, on the

basis of these thermal studies Zinc stannate cubic spinel were synthesized by calcining the SnO_2 powder and ZnO rod mixture at 1000^oC[16]. The detection of different gas by sensors of resistance-type is mainly based on the principle of varying electrical conductivity during expose to a rare gas of very low concentration in the atmosphere [17].

When a gas sensor of Zinc stannate-based is exposed to atmosphere O_2 gets adsorbed on the Zn_2SnO_4 surface, because oxygen has a strong electronegativity which traps the free electrons from the conduction band of Zn_2SnO_4 and thus adsorption of oxygen species are induced. Consequently, the resistance of gas sensing device increases due to the decreases in electrons density in the conduction band [18].

It has been reported that when a sensor based on Zn_2SnO_4 tested with gaseous environment like CO or H_2, SnO^- sites adsorbed CO molecules on surface to form carboxyl CO_2^- or carbonate group CO_3^{2-}, while molecules of hydrogen were adsorbed on Zn sites rather than on Sn sites, it resulted in the reaction of oxygen with hydrogen to produce water molecules, therefore above 350^oC, conductivity of Zn_2SnO_4-based sensor increased due to desorption of CO_2 or H_2O molecules into gaseous phase which returns free electrons[19].

The resistance of an n-type semiconductor changes when there is any gas molecules adsorption or desorption of on the sensing material's surface, and there is rapid change in gas sensitivity with the reducing particle size. The gas sensitivity of sensing material increases when size of the particle is reduced to nanoscale [20-21]. In sensing materials consolidated from rough Zn_2SnO_4, the combination of the nanoparticles become inevitable and irreversible due to strong Van der Wall's attraction between nanoparticles. [22]

Liu et al. reported the method of synthesis of Zn2SnO4/SnO2 hollow sphere by heat treating ZnSn(OH)6 spheres at 600 μC in atmosphere. Which causes the formation of Zn2SnO4/SnO2 composites with hollow spheres and as an electrode material in DSSCs, these hollow spheres have very good efficiency (4.52%) [23].

Wang et al. synthesized macro porous Zn_2SnO_4 of nanoparticles in the presence of a template called polystyrene (PS) through a hydrothermal method followed by the process of annealing. The photovoltaic performance of pore having smaller size of Zn_2SnO_4 is more, which is due to the loading of higher dye, high rate of transport and slower electron rate of recombination of electron which are confirmed by characterizing with UV-Visible photocurrent spectroscopy,

absorption spectroscopy, with intensity modulation, electrochemical resistance spectroscopy and intensity-modulated photovoltage spectroscopy [24].

Shi et al. fabricated highly ordered Zn_2SnO_4 nanotubes via a convenient hydrothermal approach by using a ZnO nanorod array as the template. The tips of the as-prepared nanotubes are all round sealed and the wall thickness of the nanotubes is about 20 nm. They showed that the shape evolution from ZnO nanorods to Zn2SnO4 nanotubes could be driven by the Kirkendall effect by studying the time-dependent reaction results. The Zn_2SnO_4 nanotubes were found to have highly efficient photocatalytic activity [25].

Hwang et al. developed a unique strategy for fabricating hierarchically structured (nanoparticles-in-beads) Zn_2SnO_4 beads (ZTO-Bs), which were then used to produce ternary metal oxide-based dye-sensitized solar cells (DSSCs). DSSCs were fabricated using the ZTO-Bs as the photoelectrodes and highly absorbable organic dyes as the sensitizers. The optimized DSSCs exhibited a power conversion efficiency of 6.3% (V_{OC} of 0.71 V, J_{SC} of 12.2 mA cm^{-2}, FF of 0.72), which was much higher than that for DSSCs with conventional ZTO-NPs-based photoelectrodes or those based on the popular ruthenium-based dye, N719 [26].

CHAPTER – 3

DIFFERENT METHODS USED TO SYNTHESIZE ZINC STANNATE POWDER

3.1 Solid State Route

Chemical reactions between solid powder precursors, usually in the form of mixed powders, are common for the synthesis of powders of complex oxides such as titanates, ferrites, and silicates. Simple oxides are the reactants such as, nitrates, sulfates, acetates, carbonates, or oxalates. An example is the reaction between zinc oxide and stannic oxide to produce zinc stannate:

$$2ZnO + SnO_2 \longrightarrow Zn_2SnO_4 \qquad (2\text{-}2)$$

This synthesis route employs the following procedure to synthesize the complex oxide powder. A mixture of the reactants mixed and milled for several hrs. After drying the mixed sample, the mixture is calcined at desired temperature and the product (powder sample) is collected after calcination. The powder characteristics depend on the heating duration and calcination temperature.

3.1 Molten Salt Synthesis.

There are various synthesis routes for the fabrication of ceramic powder, molten salt method is one among them. This method uses the molten salt as a reaction media for the fabrication of ceramic powders at a lower temperature (eutectic temperature) than the solid state method. Ceramic powders are synthesized from all the phases by various methods. Solid phase is used to synthesize various ceramic powders for commercial and industrial production by a traditional powder processing method. Traditional method is modified to form molten salt synthesis method where eutectic mixture of different salt is added to the reactant oxides and heated above melting point of the of eutectic mixture.

In solid state reactions, molten salts generally used to act as additives which improve the reaction rate. The amount of salt used as additive in solid state reaction is small but in molten salt synthesis a large amount of salt is added to the reactants. Molten salt synthesis method uses various type of salt mixture such as sulfates and chlorides. Generally to produce liquid phase temperature eutectic salt mixtures are used. For example NaCl and KCl melts at 801 and 770^{O}C, respectively, while the eutectic salt composition of NaCl-KCl (0.5NaCl– 0.5KCl) melts at 650^{o}C. For example, among sulfates $0.635Li_2SO_4–0.365Na_2SO_4$ is the most commonly used due to its low temperature melting at 594^{o}C, Eutectic mixture of different salts melts at different temperature. $Na_2SO_4–K_2SO_4$ forms liquid phase at 823^{o}C. The reaction of formation typically

occurs in existence of reactant particles. Though molten salt is added as a solvent, it is different from other normal solvents, which used to dissolve all the solid particles of oxides and precipitate the product from a homogeneous liquid phase.

The procedure of molten salt synthesis method to produce complex oxide is as followed. The eutectic mixture of salt is added to the reactant powder and mixed then the mixture is heat treated above the melting point of eutectic composition of salt. Product particles start to form at the melting temperature, where the salt starts to melt. The powder characteristic can be easily controlled by the selection of calcination temperature and heating duration. Then, the solid reacted mass formed is cooled down to room temperature and salt is removed by washing with a suitable solvent of salt followed by drying. After drying powder product is obtained.

As shown in the phase diagram the eutectic mixture of NaCl-KCl melts at 657^{o}C.

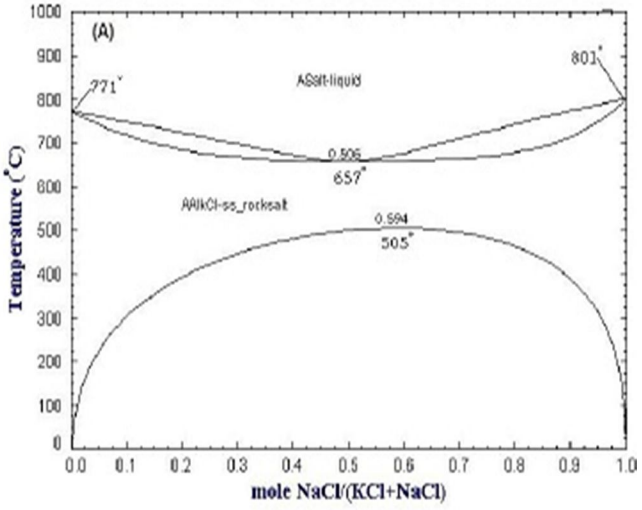

Figure 7. Phase diagram of NaCl-KCl salt system [27]

CHAPTER – 4

EXPERIMENTAL PROCEDURE

4.1 Powder Synthesis

4.1.1 Powder Synthesis by Solid State Route

ZnO (Assay = 99.5%, SRL) and SnO_2 (Assay = 99.9%, Loba Cheme Pvt. Ltd) were used as the precursor material. Stoichiometric amounts of ZnO and SnO_2 were taken and milled for 6h using polyethylene jar in propanol medium and Zirconia balls as grinding media. After milling, the slurry is transferred to a clean petri dish and kept in the oven at 100^{o}C until all the propanol got evaporated. The dried powder was taken and ground in a mortar and pestle for about half an hour and then the powder was transferred to alumina crucible and calcined at various temperatures (1000-1200^{o}C/4h).

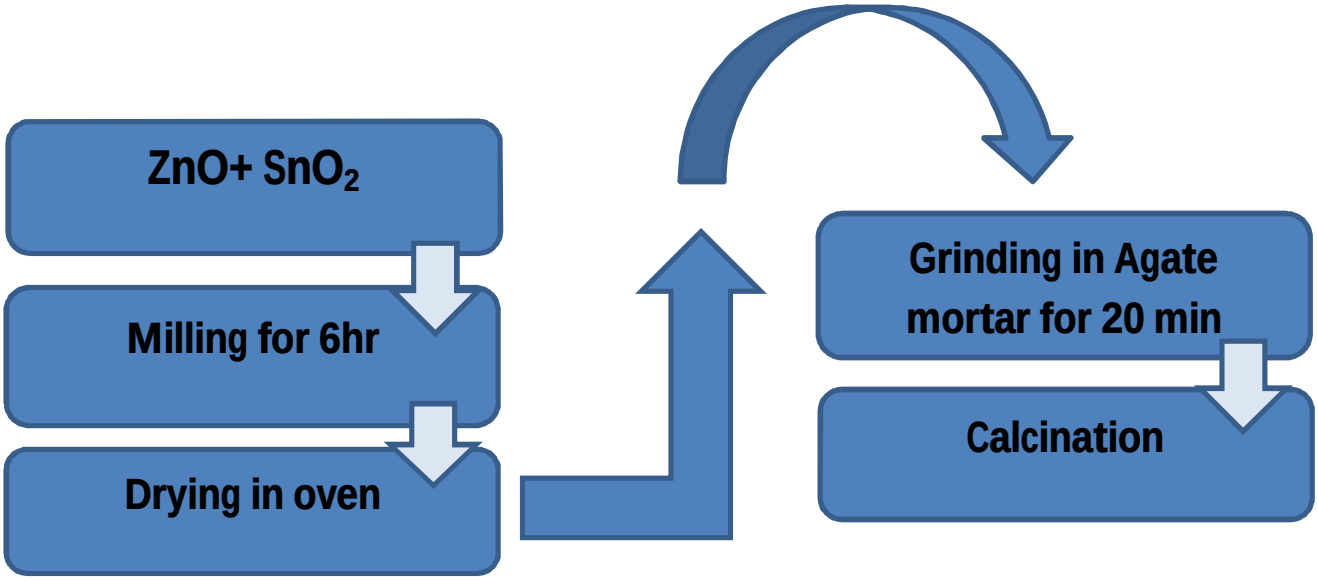

Figure 8 Flow chart of solid state synthesis route

4.1.2 Powder Synthesis by Molten Salt Method

Reagent grade ZnO, SnO_2, NaCl, and KCl were used as precursor materials. Stoichiometric amount of ZnO, SnO_2 powders were mixed with eutectic composition of NaCl-KCl (50:50) in the molar ratio of 2:1:20 to 2:1:50. The powder mixtures were homogeneously mixed using reagent grade isopropyl alcohol in an agate mortar. The mixture was then put into an alumina crucible and heat treated at 700-900^{o}C for 4 h. Then calcined powders were washed with hot deionized water until no Cl^- was detected by using $AgNO_3$ solution. The powder was dried in an oven at 100^{o}C.

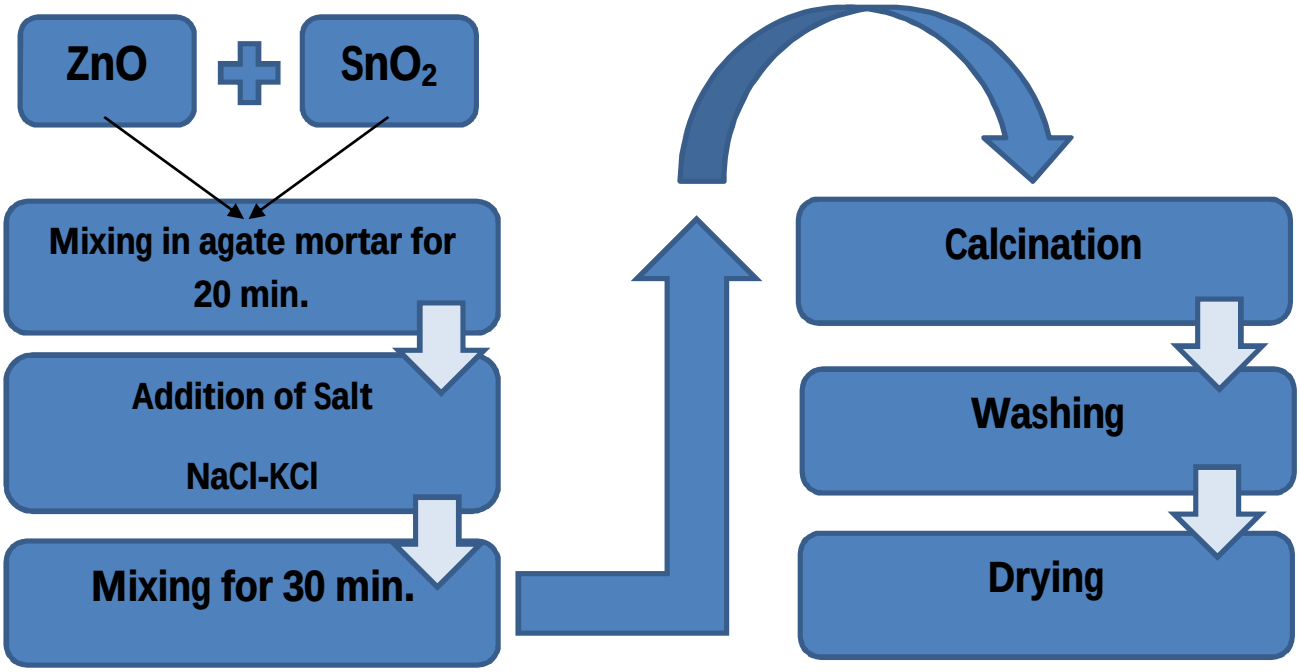

Figure 9 Flow chart for the preparation of Zn_2SnO_4 by molten salt synthesis method

4.2 Characterizations

4.2.1 Phase analysis (X-ray Diffraction)

The phase evolution of the Zinc Stannate powder was structurally characterized by X- Ray Diffraction Technique (Rigaku, Japan). Scanning of powder samples was done between a 2Ɵ ranges 15 to 80^{o} range in continuous mode of sanning with a scanning rate 20 deg/sec. The phases present in the samples was identified by the search-match facility available with Philips X`Pert High Score Software.

4.2.2 DLS Particle size analysis

A diffraction method where laser beam is used for scattering and particle size distribution of the powder is determined by multiple scattering techniques. Fraunhofer diffraction of light is caused by the dispersed particles by traversing a collimated light beam external of the cross section of the x-ray beam when the wavelength of the light is smaller than particles. The diffracted light intensity was found Proportional Square of the size of particle, while the diffraction angle varies inversely with particle size. For the light source a He-Ne laser was used. The computation of particle size distribution of sample from the raw diffraction data is due to combination of a lens, an optical filter, and photo detector or a multi element detector and lens coupled with a computer enables to do so. Liquid or gas suspension of particles or droplets of about 0.1 vol % concentration is used as sample. It is based on the theory of Mie-scattering. In order to detremine the particles size distribution, a little amount of Zn_2SnO_4 powder was dispersed in 20-40 ml of water for 15 min in an ultrasonic processor. [Ultrasonic Processor Sonopros, PR1000 MP]. The rest of the experiment was carried out in computer controlled particle size analyzer [ZETA Sizers Nanoseries (Malvern Instruments Nano ZS)] to determine the particles size distribution.

4.2.3 Field Emission Scanning Electron Microscopy (FESEM)

FESEM is a typical electron microscope which shows the powder morphology images formed by elctron beam scanning. The interaction between surface atoms and the electrons (secondary electrons (SE), back scattered electrons (BSE), characteristic X-rays initiate to produce relevant information of powder sample about microstructure, distribution of pore, morphology, and pore shape. The microstructural characteristic of Zn_2SnO_4 powder samples was elucidated using scanning electron microscope (Nova Nano SEM - 450).

4.2.4 UV-Vis Spectroscopy

Ultraviolet-visible spectroscopy (UV/ VIS) involves the photons spectroscopy in the region of UV-visible. The method uses visible light and adjacent near ultraviolet (UV) ranges. In between this region of electromagnetic spectrum, electronic transitions of molecules undergo. Diffuse reflectance spectrum of the samples have to be recorded with a UV-Vis (Lamda 25, Perkin Elmer, USA) in normal condition and room temperature. The absorbance vs wavelength was plotted and the absorbance value was revealed. The value of band gap of the ZTO powder was estimated by extrapolating the linear portion like tangent to the Tauc's plot obtained by using Kubelka-Munk relation where f(R), R, k, s denotes Kubelka-Munk function, absolute reflectance, molar absorption coefficient and scattering coefficient respectively.

The Kubelka-Munk Equation is given as follows.

$$f(R) = \frac{(1-R)^2}{2R} = \frac{k}{s}$$

CHAPTER 5

RESULTS AND DISCUSSION

5.1 Characterization of precursor powder

5.1.1 Phase analysis

Fig – 10 shows the XRD patterns of ZnO and SnO_2. All the detectable peaks could be matched with the ZnO (wurtzite structure) and SnO_2 (rutile structure) standard reference data JCPDS No: 36–1451, 41-1445 for ZnO and SnO_2 respectively.

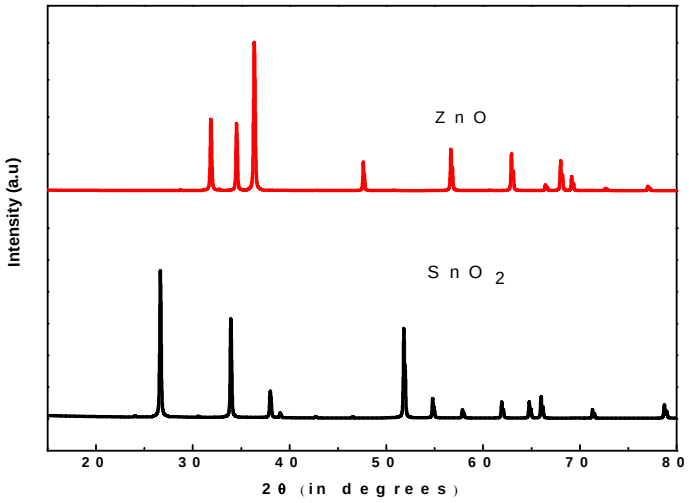

Figure 10. XRD pattern of SnO_2 and ZnO

5.1.2 Particle size analysis

Fig – 11 shows the particle size distribution of ZnO and SnO_2. From the figure it can be observed that both ZnO and SnO_2 show a broad range of particle size distribution. For ZnO, 95 vol% of the particles lies in the range of 0.6-1.1 μm. The average particle size calculated is 0.8 μm. Further, for SnO_2 95 vol% of particles are in the range 0.6-1.28 μm, the mean particle size calculated is 0.93 μm.

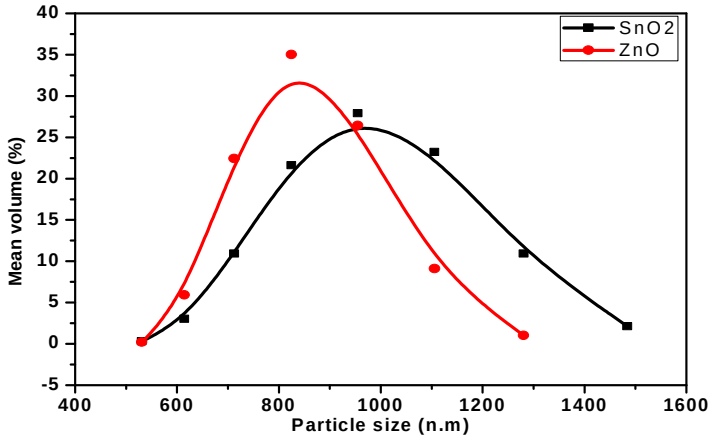

Figure 11. Particle size distribution of precursor powders

5.1.3 FESEM

The FESEM photographs of powder precursor SnO_2 and ZnO reveals the mean particles size of 0.17µm and 0.27 µm respectively. As seen from the figure the particles of SnO_2 and ZnO are having spherical to irregular shape. Particle size distribution measured by DLS technique provides only agglomerate size of the powder. The difference between the particle size values determined form the DLS and that measured by other technique may be due to agglomeration of the powder.

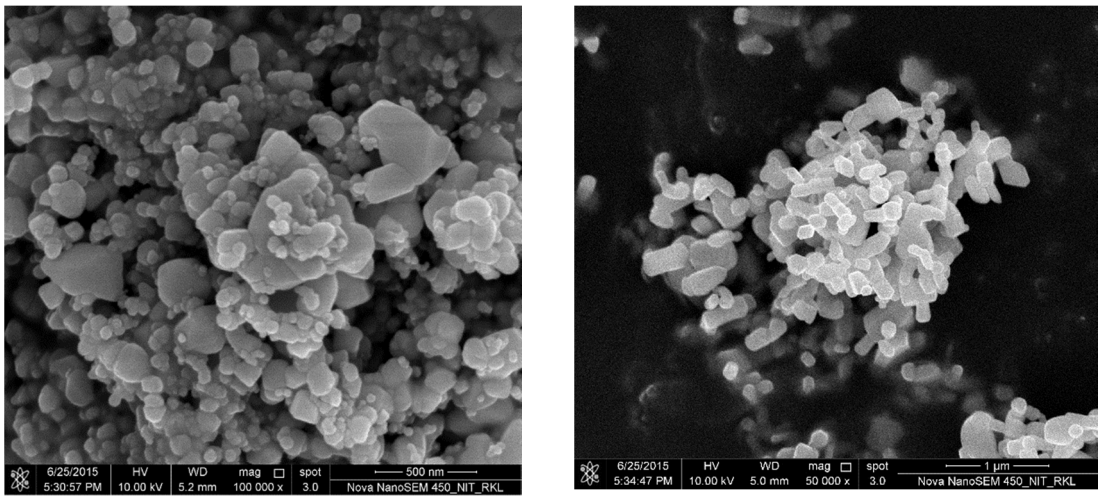

Figure 12. FESEM micrograph of SnO_2 and ZnO (from left to right)

5.2 Zinc stannate powder preparation by Solid State route

Zinc stannate powder was successfully synthesized by calcining the powder mixture of SnO_2 and ZnO at 1100 and 1200^{o}C/4h and following characterizations were done.

5.2.1 Phase Analysis

Fig – 13 shows the XRD patterns of the Zinc Stannate powder samples calcined at 1100 and 1200°C for 4h. From fig-5.4, it can be observed that all diffraction peaks of the powder samples are consistent with the JCPDS (74-2184) data of the pure inverse-spinel Zn_2SnO_4.

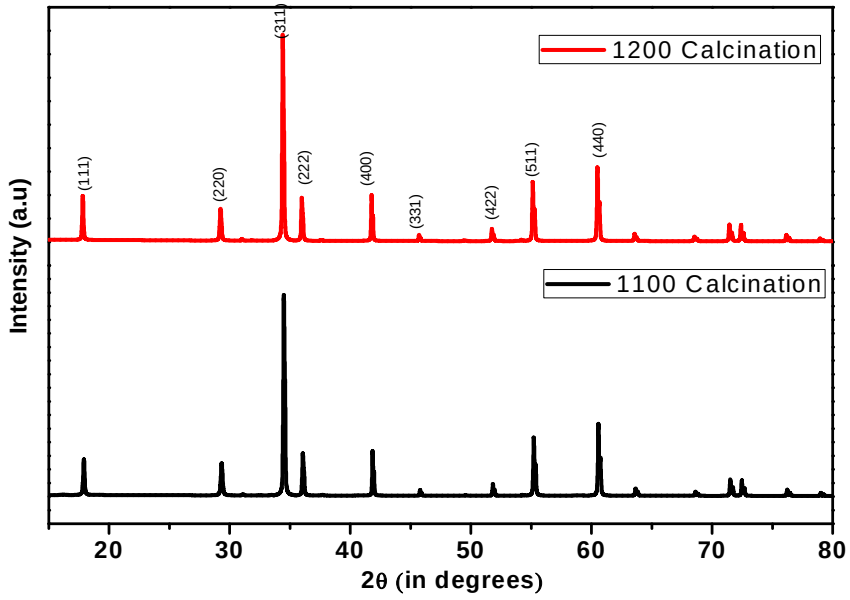

Figure 13. XRD pattern of Zn_2SnO_4 samples calcined at different temperatures

5.2.2 FESEM

Fig 14 shows the FESEM micrograph of the samples calcined at 1100 and 1200°C for 4 h. As seen from the micrograph, the particles are in irregular shape and agglomerated. The average particle size increased with the increase of calcination temperature. The average particle size of Zn_2SnO_4 particles calcined at 1100 and 1200°C/4h are 0.23 and 0.25 μm, respectively.

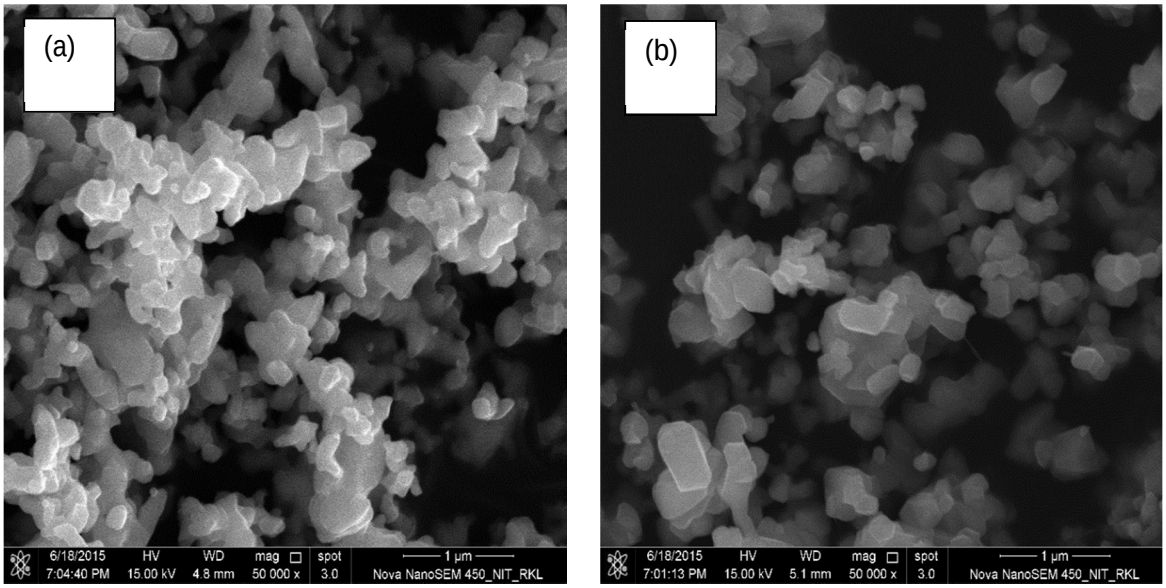

Figure 14.FESEM images of Zn2SnO4 calcined at a) 1100 and b) 1200^{o}C for 4h respectively

5.2.3 UV-Visible

The diffuse reflectance spectra were recorded [Fig.15 (a)] in the wavelength range of 200–1000 nm for the samples heat treated at 1100^{o}C and 1200^{o}C. The Kubelka Munk function [28] as given below was used to determine the optical band gap of Zn_2SnO_4 powders.

Fig. 15(b) shows the plot of $[F(R)h\upsilon]^{1/2}$ versus $h\upsilon$ from which the band gaps of Zn_2SnO_4 powders are evaluated by extrapolating the linear portions of the curves. The Zn_2SnO_4 powder exhibited a band gap of 2.9, whereas the other sample calcined at 1200^{o}C has the band gap around 3.0 eV (Fig. 15-16). The value of the band gap slightly decreased compared to the literature reported value 3.5 eV as reported in the above literature, which may be due to the formation of oxygen vacancies during high temperature sintering.

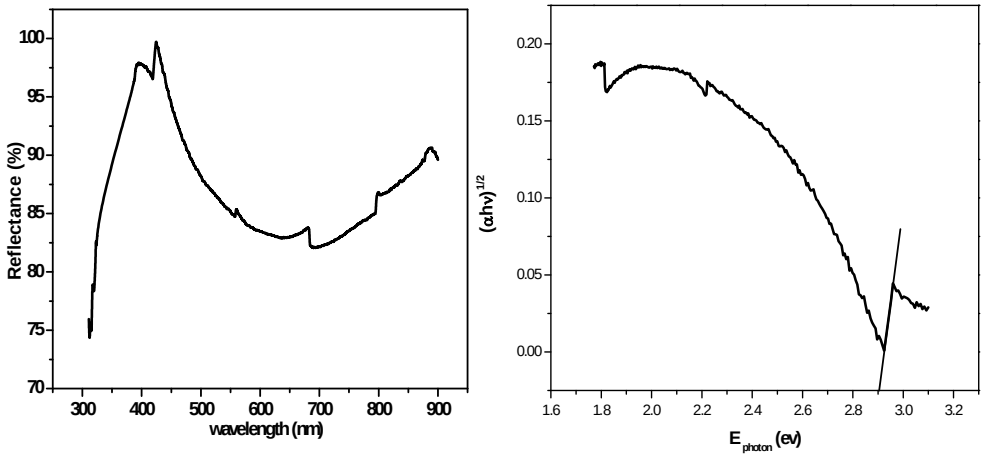

Figure 15. (a) Reflectance Spectra of Zn2SnO4 calcined at 1100^{o}C (b) Tauc plot

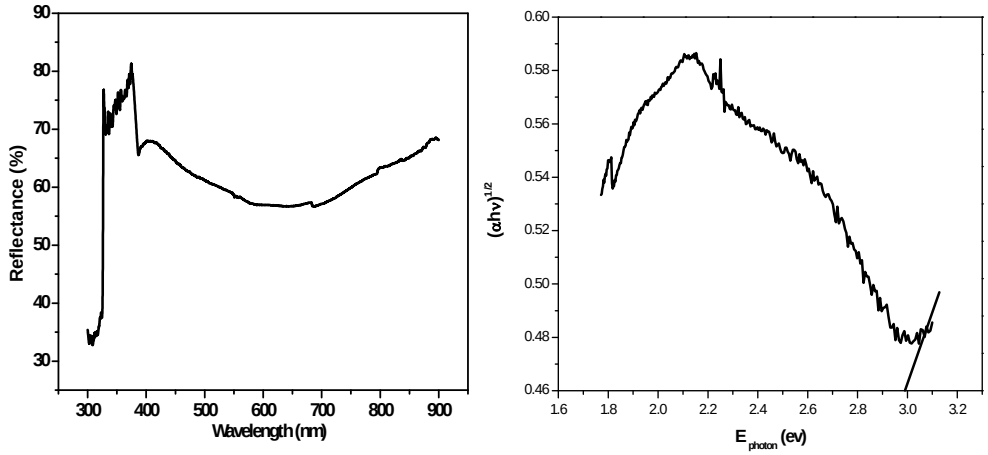

Figure 16 (a) Reflectance Spectra of Zn_2SnO_4 calcined at 1200°C (b) Tauc plot

5.3 Molten Salt Synthesis

Molten salt synthesis of Zn_2SnO_4 was done in two steps. In the first step, the salt content (NaCl-KCl) was kept constant (2:1:20) and calcined at different temperature (700-900°C). In the second step calcination temperature was maintained constant at 900°C and the molar ratio of salt was varied from 2:1:25 to 2:1:50.

5.3.1 Phase analysis

Fig 17 shows the XRD pattern of Zn2SnO4 powder synthesized by molten salt method. It can be observed that with increase in calcination temperature no significant change can be observed.

Only 7% of Zn_2SnO_4 phase is formed, which is well matched with the standard JCPDS No. 74-2184.

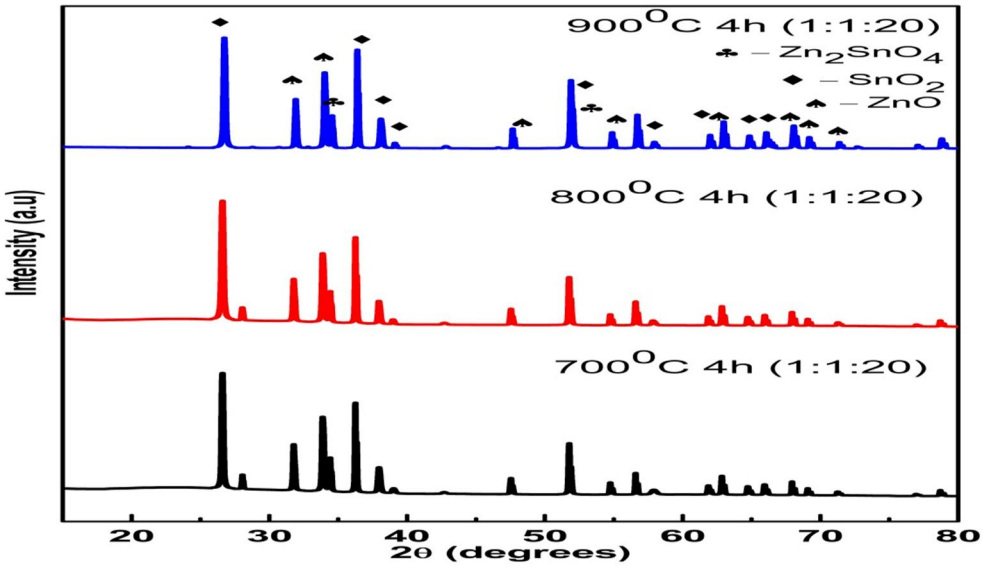

Figure 17. XRD pattern of powder synthesized by molten salt method with varying calcination temperature

Fig 18 shows the XRD pattern of Zn_2SnO_4 synthesized by molten salt Method by varying salt content keeping calcination temperature fixed at 900^0C. From the figure it was observed that with increase in salt content there is no significant change in the amount of Zn_2SnO_4.

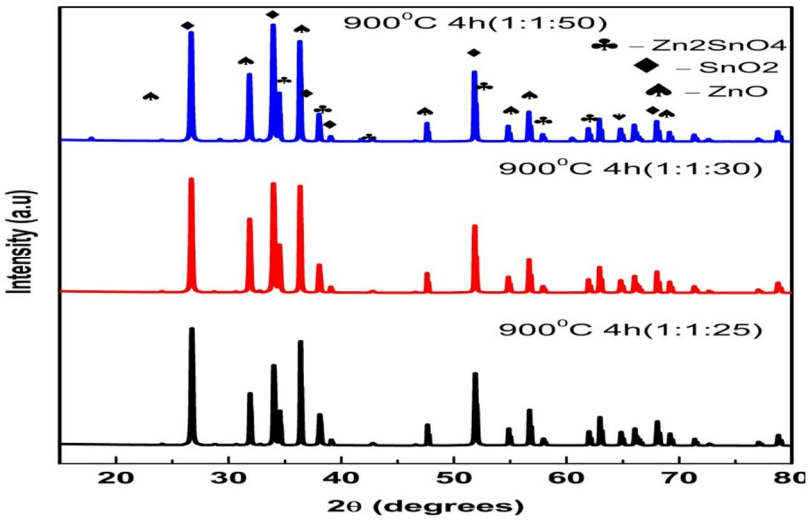

Figure 18. XRD pattern of powder synthesized by molten salt method with varying salt content

5.3.2 DLS (particle size analysis)

The graph shows particle size distribution of Zn_2SnO_4 powder calcined at 900^oC which shows us a broad particle size distribution with 97 vol% of the particles lying in the range 295-650 nm. The mean particle size calculated to be 522 nm.

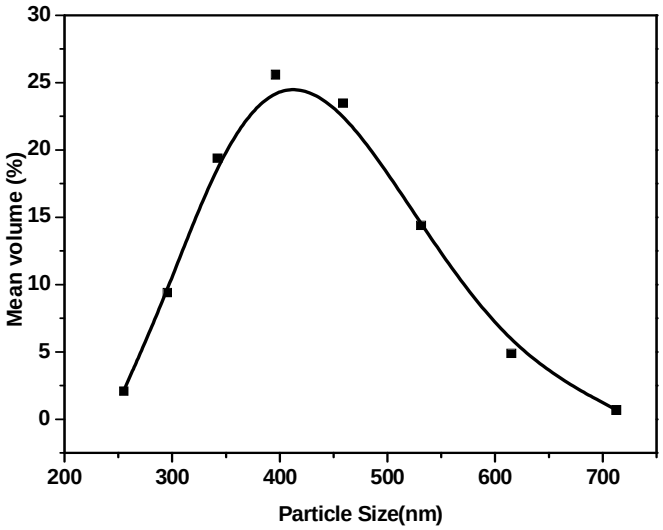

Figure 19 PSD of Zn_2SnO_4 powder calcined at 900^oC

5.3.3 FESEM

Fig 20 shows the FESEM micrograph of Zn_2SnO_4 composite powder at salt content 2:1:25. The image shows that powders are irregular in shape and the mean particle size was found to be 0.32µm.

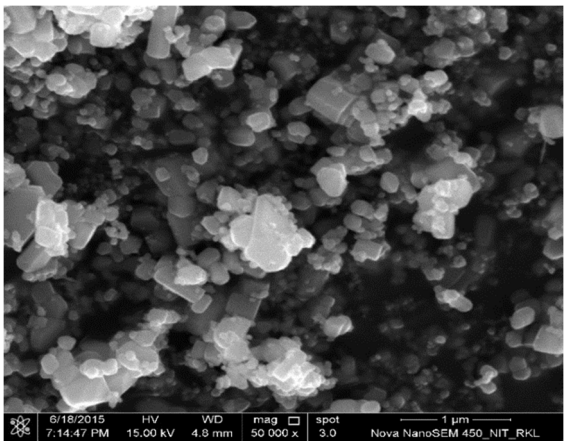

Figure 20 FESEM image of Zn2SnO4 calcined at 900°C by molten salt method

5.3.4 UV Visible

Fig. 21(a) shows the diffuse reflectance spectra of the Zn_2SnO_4 composite powder in the wavelength range of 200–1000 nm for the samples prepared at salt content 2:1:25 and fired at 900°C. Fig. 21(b) shows the plot of $[F(R)h\upsilon]^{1/2}$ versus hυ from which the band gaps of Zn_2SnO_4 composite powder was found to be 2.95 eV and there is a high absorbance at 350 - 400 nm range. The absorbance curve shows a narrow range of absorbance.

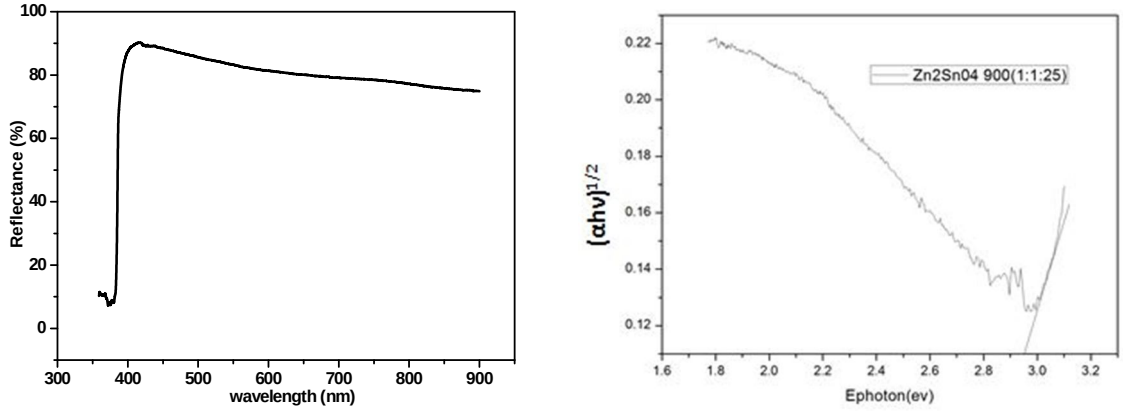

Figure 21 (a) Reflectance Spectra of powder calcined at 900°C by molten salt method (b) Tauc plot

CONCLUSION

- Zn_2SnO_4 powder was successfully synthesized by solid state route. Phase purity was obtained at 1200^oC.
- From the FESEM micrographs the mean particle size of zinc stannate powder calcined at 1100 and 1200^oC was found to be 0.23 and 0.25 μm, respectively.
- The band gap of zinc stannate calcined at 1100 and 1200^oC was calculated from the tauc plot and the values are found to be 2.9 eV and 3.0 eV respectively.
- In molten salt synthesis maximum 7-10 wt% of zinc stannate phase was obtained. The FESEM graph of molten salt composition (1:1:25) calcined at 900^oC shows the mean particle size of 0.32μm.
- The band gap of zinc stannate composite composition was calculated to be 2.9 eV.
- It can be concluded that NaCl-KCl based molten salt synthesis is not suitable for synthesis of zinc stannate.

REFERENCE

[1]. T. J. Coutts, D. L Young, X Li, W. P Mulligan, X. J Wu. Vac. Sci. Technol. A 2000, 18, 2646.

[2]. Rongmei Liu, Wei Du, Qun Chen, Feng Gao, Chengzhen Wei, Jing Sun and Qingyi Lu RSC Adv, 2013, 3, 2893.

[3]. J. Zeng, M.D. Xin, K.W. Li, H. Wang, H. Yan, W.J. Zhang, J. Phys. Chem. 2008, C 112, 4159-4167.

[4]. D. Brida, E. Fortunato, I. Ferreira, H Aguas, R Martins. J. Non-Cryst. Solids. 2002, 299, 1272–1276.

[5]. T. Hashemi, H. M. Al-Allak, J. Illingsworth, A. W. Brinkman and J. Woods, J. Matter. SCi Lett 1990, 9, 776; I. Stanboloya, A.Toneva, V.Blaskov, D. Radev, Ya. Tsvetanova, S. Vassilev and P. Peshev, J. Alloys Compd., 2005, 391, L1; J.-W. Zhao, L.-R. Qin, and L.-D. Zhang, Solid State Commun, 2007, 141, 663.

[6]. H. Hou, Q. Cheng, Y. Bhai and W. F. Xhang, Solid State Ionics, 2010, 181,1631

[7]. (a) Toshio Kimura, 2011, DOI: 10.5772/20472, (b)Ganesh K Sahoo, M.Tech Thesis, NIT Rourkela, 2009, Synthesis and characterization of $BaTiO_3$ Prepared by Molten Salt Synthesis Method.

[8]. Zhe Chen, Minhua Cao, and Changwen Hu, J. Phys. Chem. C, 2011, 115 (13), 5522–5529.

[9]. K. Jeyadheepan and C. Sanjeeviraja, journal of chemistry. Olume 2014, Article ID 2405918.

[10]. Ü. Özgür,Ya. I. Alivov, C. Liu, A. Teke, M. A. Reshchikov, S. Doğan, V. Avrutin,S.-J. Cho, and H. Morkoç, Journal of Applied Physics (Impact Factor: 2.19). 08/2005; 98(4):041301-041301-103.

[11]. C. H. drake, Understanding the low temperature electrical properties of nanocrystalline sno_2 for gas sensor applications; Journal of Research Gate, 01/2007.

[12]. Zhe Chen , Minhua Cao , and Changwen Hu , J. Phys. Chem. C, 2011, 115 (13), 5522–5529.

[13]. V. Sepelak, S. M. Becker, I. Bergmann, S. Indris, M. Scheuermann, A. Feldhoff, C. Kubel, M.l Bruns, N. Sturzl, A. S. Ulrich, M. Ghafari, H. Hahn, C. P. Grey, K. D. Becker , P. Heitjans , J. Mater. Chem., 22, 2012, 3117-3126.

[14]. L. C. Nehru, C. Sanjeeviraja, Nanoscience and Nanotechnology 2013, 3(1): 10-13.

[15]. Nader Ghobadi, International Nano Letters 2013, 3:2, doi: 10.1186/2228-5326-3-2.

[16]. J.H. Lee, Sens. Actuators. 2009, B 140, 319-336.

[17]. B.K. Kim, S.D. Choi, Sens. Actuators. 2004, B 98, 239-246.

[18]. T. Tharsika, A.S.M.A Haseeb, S.A. Akbar, Mohd Faizul Mohd Sabri,Yew Hoong Wong, journal of Alloys and Compounds 2015, 618, 455–462

[19]. J.H. Yu, G.M. Choi, J. Electroceram. 2002, 8, 249-255.

[20]. Y.L. Wang, X.C. Jiang, Y.N. Xia, J. Am. Chem. Soc. 2003, 125, 16176-16177.

[21]. J.H. Lee, Sens. Actuators. 2009, B 140, 319-336.

[22]. B.K. Kim, S.D. Choi, Sens. Actuators. 2004, B 98, 239-246.

[23]. Rongmeim Liu, Wei Du, Qun Chen,Feng Gao, Changzhen Wei, Jing Sun and Qingyu, Lu. , DOI: 10.1088/0256-307X/29/5/056801.

[24]. Yu-Fen Wang, Ke-Nan Li, Yang-Fan Xu, Hua-Shang Rao, Cheng-Yong Su and Dai-Bin Kuang, Nanoscale, 2013, 5, 5940-5948.

[25]. Liang Shi and Yumei Dai, J. Mater. Chem. A, 2013, 1, 12981.

[26]. D. Hwang, J.-S. Jin, Horim Lee, Hae-Jin Kim, Heejae Chung, Dong Young Kim, Sung-Yeon Jang & Dongho Kim Scientific Reports | 4: 7353 | DOI: 10.1038/srep07353.

[27]. Ganesh K Sahoo, M.Tech Thesis, NIT Rourkela, 2009, Synthesis and characterization of $BaTiO_3$ Prepared by Molten Salt Synthesis Method.

[28]. Kubelka and Munk, Zeit. Für Tekn. Physik, 12, 593 (1931).